An assessment of microwave absorption models and retrievals of cloud liquid water using clear-sky data

Roger Marchand,[1] Thomas Ackerman,[1] Ed R. Westwater,[2] Shepard A. Clough,[3] Karen Cady-Pereira,[3] and James C. Liljegren[4]

Received 7 June 2003; revised 10 August 2003; accepted 5 September 2003; published 19 December 2003.

[1] Passive microwave radiometers have a long history in the remote sensing of atmospheric liquid and water vapor. Retrievals of these quantities are sensitive to variations in pressure and temperature of the liquid and water vapor. Rather than use a statistical or climatological approach to account for the natural variability in atmospheric pressure and temperature, additional information on the atmospheric profile at the time of the radiometer measurements can be directly incorporated into the retrieval process. Such an approach has been referred to in the literature as a ''physical-iterative'' solution. This paper presents an assessment of the accuracy of the column liquid water path that can be expected using such an iterative technique as a result of uncertainties in the microwave emissions from oxygen and water vapor. It is shown that the retrieval accuracy is influenced by the accuracy of the instrument measurements and the quality of the atmospheric profiles of temperature and pressure, as one would expect. However, also critical is the uncertainty in the absorption coefficients used in the underlying microwave radiative transfer model. The uncertainty in the absorption coefficients is particularly problematic in that it may well bias the liquid water retrieval. The differences between three absorption models examined in this paper are equivalent to a bias of 15 to 30 g/m^2, depending on the total column water vapor. An examination of typical liquid water paths from the Southern Great Plains region of the United States shows that errors of this magnitude have significant implications for shortwave radiation and retrievals of cloud effective particle size. *INDEX TERMS:* 0360 Atmospheric Composition and Structure: Transmission and scattering of radiation; 0394 Atmospheric Composition and Structure: Instruments and techniques; 3360 Meteorology and Atmospheric Dynamics: Remote sensing; 6904 Radio Science: Atmospheric propagation; *KEYWORDS:* microwave radiometry, cloud liquid water

Citation: Marchand, R., T. Ackerman, E. R. Westwater, S. A. Clough, K. Cady-Pereira, and J. C. Liljegren, An assessment of microwave absorption models and retrievals of cloud liquid water using clear-sky data, *J. Geophys. Res.*, *108*(D24), 4773, doi:10.1029/2003JD003843, 2003.

1. Introduction

[2] Passive microwave radiometers have a long history in the remote sensing of atmospheric liquid and water vapor [*Westwater*, 1978; *Hogg et al.*, 1983]. By measuring the emission of microwaves by the atmosphere at two or more frequencies, one can estimate the amount of liquid water and water vapor present in the atmospheric column. The intensity of the microwave emissions, usually expressed as an equivalent temperature at which a blackbody would radiate the same amount of energy, depends on the temperature and pressure of the liquid and water vapor and hence their location in the atmospheric column.

[3] One approach to handle the variability in the atmospheric temperature and pressure is to use a statistical approach [*Westwater*, 1993]. In the statistical approach, a set of radiosonde profiles of the atmospheric thermodynamic state (for a given area and for a given time of year) are used as input to a microwave radiative transfer code that is able to calculate the microwave brightness temperature which would be measured by a microwave radiometer. A linear regression is then used to model the relationship between the atmospheric opacity at these microwave frequencies and the total vapor and liquid water, which was used as input to the radiative transfer model. (The atmospheric opacity is a function of the measured brightness temperatures and the mean radiating temperature of the atmosphere, both of which are calculated by the microwave radiative transfer code.) This regression relationship (combined with the mean radiating temperature of the atmosphere for that

[1]Pacific Northwest National Laboratory, Richland, Washington, USA.
[2]Cooperative Institute for Research in Environmental Sciences, University of Colorado/NOAA Environmental Technology Laboratory, Boulder, Colorado, USA.
[3]Atmospheric and Environmental Research, Lexington, Massachusetts, USA.
[4]Environmental Research Division, Argonne National Laboratory, Argonne, Illinois, USA.

0148-0227/03/2003JD003843$09.00

location) then forms the basis of retrieving the total vapor and liquid water from actual measurements of the brightness temperature.

[4] The U.S. Department of Energy, as part of its Atmospheric Radiation Measurement (ARM) Program, has deployed passive microwave radiometers at it field sites located in the Southern Great Plains (near Lamont, Oklahoma), North Slope of Alaska (near Barrow, Alaska), and the tropical western pacific (on the islands of Manus and Nauru). A wealth of information and data from these sites can be found at http://www.arm.gov/. Our experience with the ARM data suggests that uncertainties in the column liquid water retrievals are undesirably large for a significant percentage of boundary layer clouds. In section 2, we briefly examine the distribution of cloud liquid water and show that uncertainties in the liquid water can have a significant impact on shortwave (solar) flux calculations and associated retrievals of cloud droplet effective radius.

[5] One possible approach to improve the estimates of column liquid water over the statistical approach is to incorporate information on the atmospheric profile at the time of the brightness temperature measurements. We have written software which, given radiosonde-like profiles of temperature, pressure and the location of clouds, as well as the shape of the water vapor profile with height, solves for the column liquid water and the column water vapor. The solution is obtained by iteratively searching for values of the column liquid water and for the water vapor which, when used in a forward model, minimize the difference between the measured brightness temperatures and the forward model calculation. This approach has been referred to in the literature as a ''physical-iterative'' approach [e.g., *Han and Westwater*, 1995; *Liljegren et al.*, 2001], but we will refer to it here as simply the minimization or iterative solution. Details on the microwave radiative transfer models and our iterative scheme are given in section 3.

[6] This paper presents an assessment of the accuracy of the column liquid water path that can be expected using such an iterative technique as a result of uncertainties in the microwave emissions from oxygen and water vapor. We do not address here the uncertainty due to potential errors in the dielectric properties of water, which *Westwater et al.* [2001] have recently suggested may be a problem for supercooled water. It is shown that the retrieval accuracy is influenced by the accuracy of the instrument measurements and the quality of the atmospheric profiles of temperature, pressure and the assumed location of liquid and water vapor, as one would expect. However, also critical is the uncertainty in the absorption coefficients used in the microwave radiative transfer model. The uncertainty in the absorption coefficients is particularly problematic in that it may well bias the final results by as much as 0.5 K to 1 K (depending on the total column water vapor), which is approximately equivalent to an error of 15 to 30 g/m^2 in the liquid water path. The differences in the individual microwave absorption model components (oxygen, water vapor line, self-broadened continuum, and foreign-broadened continuum) can be larger than this but tend cancel out.

[7] This assessment is based on an evaluation of 10 carefully selected clear-sky cases, which are described section 4. How can we use clear-sky data to evaluate liquid water? The ARM microwave radiometers make brightness temperature measurements at two frequencies. Both measurements respond to both the liquid and vapor, but one channel is more sensitive to vapor and the other is more sensitive to liquid water. So, under clear sky conditions we can use one measurement to solve for the water vapor and determine if the forward calculation of the measurement in the other channel matches the measured value. Any difference between the calculation and the measurement directly reflects an error that would be introduced into the liquid retrieval if a cloud had been present. We can further evaluate this error by inserting a false cloud into the retrieval processes and observing the solution of the liquid water, all of which is error. Section 5 presents results for the 10 case study days and section 6 summaries these results and their implications for cloud liquid water path retrievals.

[8] In their examination of data from the arctic, *Westwater et al.* [2001] studied two of the three microwave absorption models used in this study. In agreement with the results presented here, these authors found a 0.5 K bias in the background oxygen component between the models and an associated bias in liquid water path retrievals. Based in part on a comparison of microwave radiometer derived liquid water paths and aircraft measurements these authors suggested that the Rosenkranz 98 model appeared to work better. Our results also suggest that the Rosenkranz model works better in the arctic than the other models, but not so at midlatitude or tropical sites.

2. Overview of Shortwave (Solar) Radiative Impact

[9] The total shortwave (solar) flux reaching the surface or reflecting back through the top of atmosphere is a nonlinear function of the cloud liquid water. Figure 1 shows a typical result for a plane parallel or one-dimensional cloud. The slope of the flux versus liquid water path curve is greatest when the liquid water path is small. Consequently, uncertainties in the liquid water path will tend to have the largest radiative impact when the liquid water path is small.

[10] Figures 2 and 3 plot errors in the downwelling flux at the surface and upwelling flux at the top of atmosphere, assuming an over-estimate in the liquid water path of 10 or 20 g/m^2. As one would expect, overestimating the liquid water path increases the cloud albedo causing the surface flux to decrease and the outgoing top of atmosphere flux to increase. If one assumes an under-estimate in the liquid water path, the results are much the same, except the signs are reversed. Figures 2 and 3 show that the error in the surface and top of atmosphere flux can be quite large, especially for liquid water paths less than 100 g/m^2. For comparison, the ARM program strives to make surface flux measurements accurate to 10 W/m^2.

[11] Figures 2 and 3 assumed a cloud with an effective radius of 10 μm. The error tends to increase as the effective radius decreases, and since most continental clouds appear to have effective radius smaller than this, these plots are a conservative estimate of the error in that sense. The sensitivity of these results to aerosols and surface albedo is generally quite small except at small values of the liquid water path ($<\sim$20 g/m^2).

[12] So, do clouds often have liquid water paths less than 100 g/m^2? Figure 4 shows the distribution of liquid water

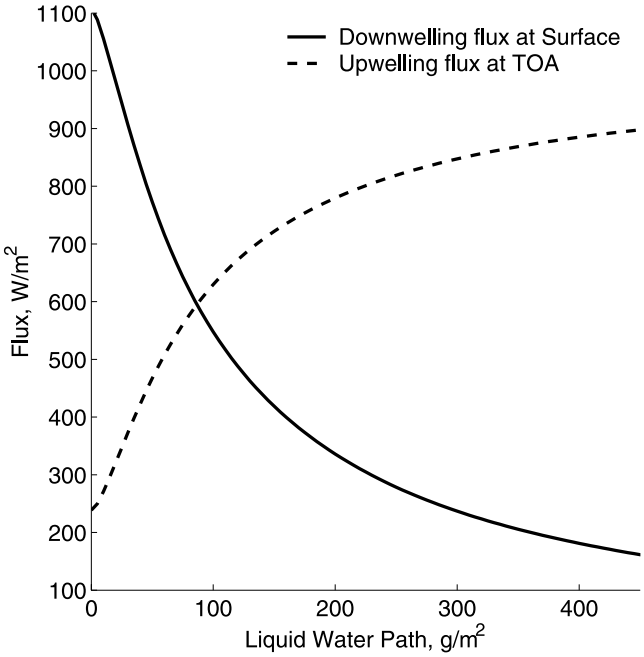

Figure 1. Example of shortwave (solar) flux reaching the surface and reflecting back through the top of atmosphere for a plane parallel cloud. In this example, the sun is directly overhead (solar zenith = 0), the cloud droplets are fixed at 10 μm, the surface is dark (albedo = 0.05 at all wavelengths), and a typical atmosphere (US72) for midlatitude conditions is assumed.

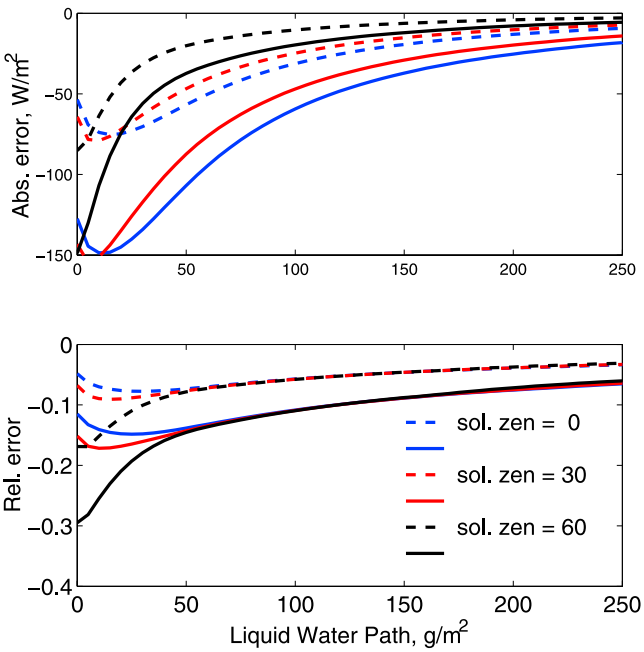

Figure 2. Error in downwelling surface flux due to a 10 g/m^2 (dashed curve) or 20 g/m^2 (solid curve) overestimate in liquid water path. (top) Absolute error (defined as the solution with error-correct solution). (bottom) Relative error (defined as absolute error/correct solution).

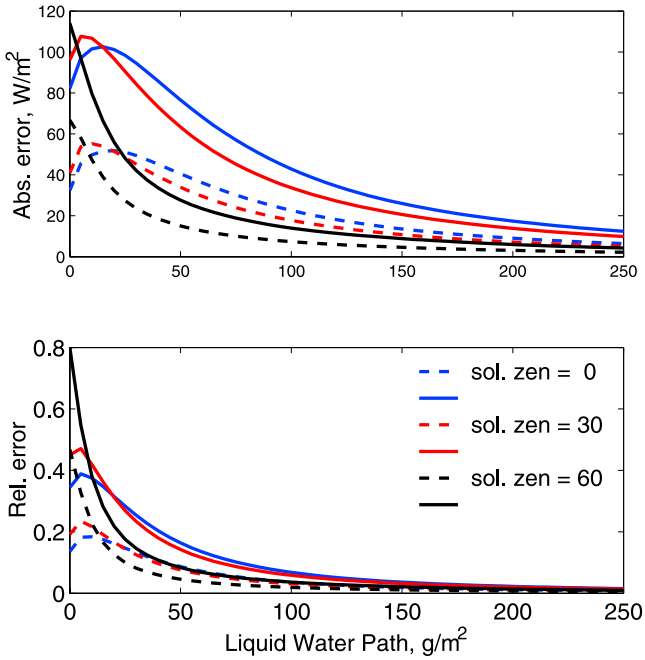

Figure 3. Same as Figure 2 except for error in upwelling flux at top of the atmosphere.

clouds estimated from microwave radiometer measurements (using the aforementioned statistical approach) from the ARM Southern Great Plains central facility near Lamont, Oklahoma. This distribution only includes measurements taken when clouds were detected by both vertically pointing radar and lidar [*Clothiaux et al.*, 2000], for a period of no less than 5 minutes (the liquid water path has been averaged on that timescale to reduce noise), and when the cloud base temperature was 5°C or larger. The cloud base temperature was inferred from a Heimann KT 19.85 Infrared Radiation Pyrometer, also known as an infrared thermometer, which is essentially a narrow-field of view IR measurement in the atmospheric window region between 9.6 and 11.5 μm. Figure 4 shows that while the mean value of cloud liquid water is reasonably large (>200 g/m^2), a significant percentage, including the peak of the distribution, have values well below 100 g/m^2.

[13] While restricting the distribution to clouds with an apparent IR temperature of greater than 5°C minimizes the influence of ice clouds, it also biases the distribution toward thicker clouds because (1) it does not include the thin altostratus and altocumulus clouds, typically containing small amounts of super-cooled water, and (2) thin clouds with low emissivities will in general appear colder than the actual cloud base temperature. It is difficult to assess how large the category of thin clouds may be. Figure 5 shows a comparison of the liquid water distributions where one distribution is restricted by the IR thermometer and the other by the location of cloud base (as determined from lidar) and then combined with the nearest-available radiosonde temperature profile to estimate the cloud base temperature (which is still required to be 5°C or greater).

[14] Keep in mind that both Figures 4 and 5 are based on the statistical retrieval, which is accurate to about 20 g/m^2 (RMS) for clouds with small amounts of liquid water. For

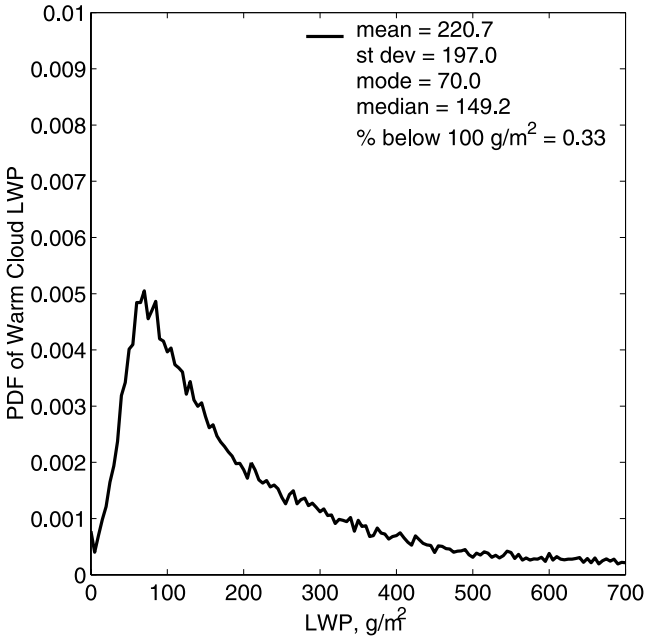

Figure 4. Probability density function of LWP for clouds with a cloud bottom IR brightness temperature of 5°C or greater and detected by both ground-based radar and lidar at the ARM program Southern Great Plain site (Lamont, Oklahoma) from December 1996 through December 2001.

comparison, Figure 6 shows the retrieved liquid water path during clear-sky periods. The mean and standard deviation shown in Figure 6 are consistent with the results given by *Liljegren et al.* [2001] and we refer the reader to this article

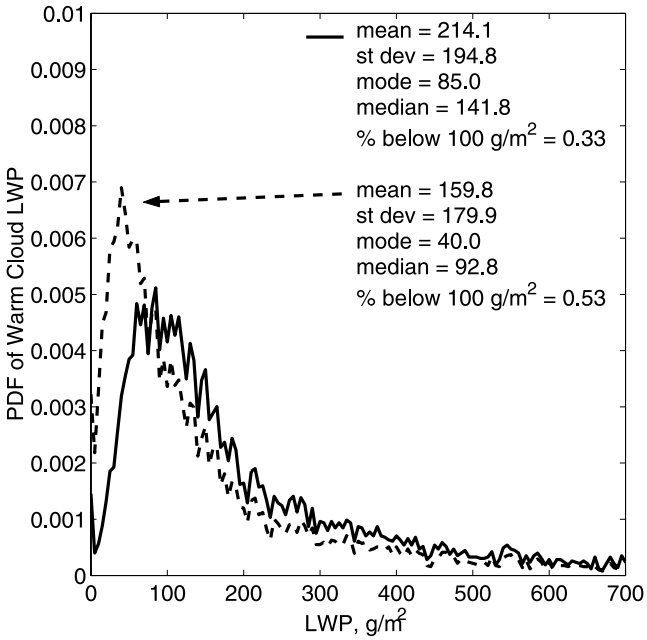

Figure 5. Probability density function of LWP. Solid curve is same as Figure 4 except restricted to 1997. Dashed curve is for all clouds (detected by radar and lidar) whose cloud base is located at a temperature of 5°C or greater when compared with the nearest available atmospheric temperature profile from radiosonde measurement.

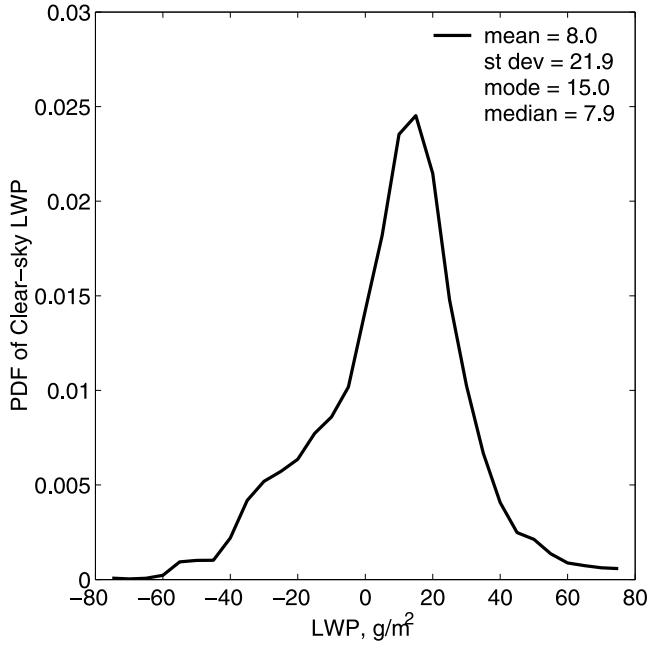

Figure 6. Probability Density Function of liquid water paths derived using the statistical retrieval during clear-sky periods for a 5 year period starting December 1996. For this figure, clear-sky means that neither radar nor lidar detected any cloud for a 3 hour period and both instruments were operating normally.

for additional discussion on the accuracy of the statistical approach.

[15] While the lidar/radiosonde approach will no doubt have included some clouds with no liquid water (owing primarily to the poor temporal and spatial coverage of the radiosonde data), it is fair to conclude that somewhere between a third to a half of all warm stratus clouds at the ARM SGP site have liquid water paths less than 100 g/m^2 - where the radiative effects of at 10 to 20 g/m^2 error is large.

[16] Of course, programs such as ARM are not generally using liquid water path retrievals to calculate surface fluxes. However, they do combine the MWR-derived liquid water path data with retrieved values of the cloud optical depth to infer the cloud drop effective radius [e.g., *Min and Harrison*, 1996; *Dong et al.*, 1997]. To a good approximation, the average cloud effective radius is given by

$$r_e = \frac{3}{2}\frac{LWP}{\tau}$$

where r_e is the effective radius, LWP is the liquid water path, and τ is the optical depth. Thus an error of 20% in the LWP (e.g., an error of 20 g/m^2 for a cloud with 100 g/m^2) will cause an error of about 20% in the retrieved effective radius.

3. Description of the Microwave Iteration Scheme and Microwave Radiative Transfer Models

[17] The iteration scheme mentioned in the introduction searches for values of the column liquid water and for the water vapor which minimize the difference between the

measured brightness temperatures and that calculated from a microwave radiative transfer model. In this study two microwave radiative transfer codes were tested. One of the radiative transfer codes was written by *Schroeder and Westwater* [1991] and the other, called is MonoRTM, was written by S. Boukabara and T. Clough [*Boukabara et al.*, 2001].

[18] All of the differences shown in this paper are due to differences in the underlying microwave absorption models, NOT the details of the radiative transfer codes. To ensure this, we modified MonoRTM to use the absorption models from the Westwater code and were able to get complete agreement between the two codes when using the same absorption model, with one minor difficulty. The Westwater code calculates the saturation vapor pressure using the Goff-Gratch formulation (formula can be found in appendix B of *Cruz-Pol et al.* [1998]), while MonoRTM uses an equation taken from LOWTRAN and claims to be accurate to 1% from +50 to −50°C. These two formulations produced column water vapor amounts that differed at the 1 to 2% level. The MonoRTM equation gives results there are very close to the equations given by *Rogers and Yau* [1989, equation (2.17)], and so for uniformity, we altered the Westwater code to use this formulation.

[19] In this study three different, but well-established, microwave absorption models were examined. The three absorption models are based primarily on the work of the *Liebe and Layton* [1987], *Rosenkranz* [1998, 1999], and MonoRTM version 2.1, hereinafter referred to as L87, R98 and MonoRTM. Each of the absorption models contain components to account for the absorption due to (1) oxygen and nitrogen, though this later term is negligibly small for the wavelengths examined herein, (2) water vapor line absorption, and (3) water vapor continuum absorption, which is further divided into a self-broadened and foreign-broadened terms.

[20] Each of the microwave absorption models contain somewhat different sub-models for each of these three components and these differences impact the overall solution at a small but significant level, as will be shown in section 5. To summarize the models briefly: The L87 model uses the equations of *Liebe* [1985] for all three of the above components with modifications and coefficients suggested by *Liebe and Layton* [1987] and includes interference coefficients for overlapping oxygen lines after *Rosenkranz* [1998]. The R98 model uses the oxygen and nitrogen model given by *Liebe et al.* [1992] and *Rosenkranz* [1993], respectively. The water vapor line absorption is based on the HITRAN database (1992) and a combination of foreign and self-broadened continuum terms from *Liebe and Layton* [1987] and *Liebe et al.* [1993]. *Rosenkranz* [1998] should be consulted for further details and analysis. MonoRTM version 2.1 uses the CKD 2.4 continuum [*Clough et al.*, 1989, 1992]. The water vapor line absorption in MonoRTM version 2.1 is based on the work of *Clough et al.* [1973]. These spectral line parameters are ∼1% below those in the HITRAN 1996 database. As a consequence, one may expect precipitable water vapor retrievals based on version 2.1 of MonoRTM to provide values that are 1% greater than those from MonoRTM version 1.0, which used values from the HITRAN database.

[21] To calculate the brightness temperature, a microwave radiative transfer code requires a profile of pressure, temperature, relative humidity and liquid water content. In this study, the pressure and temperature profiles from the nearest-in-time available radiosonde, which was launch at the radiometer site, are used. The radiosonde profile of relative humidity is also used, but is adjusted by a multiplicative factor. Choosing a factor greater than one results in a total column precipitable water vapor (PWV) larger than would be calculated from the radiosonde profile, and a factor less than one results in PWV that is less than the radiosonde value. If the multiplicative vapor factor is larger than one, and would cause the relative humidity in some portion of the profile to be larger than 100%, the relative humidity is set to 100% in that portion. In effect, the radiosonde profile determines the distribution of water vapor with height (and therefore temperature), but not the total PWV. As one would expect, the multiplicative factor is typically close to one.

[22] The ARM program operates millimeter wavelength cloud radar at all of its primary sites. In the general case, we use data from this instrument to specify a pattern for the liquid water content profile. The relative humidity in the cloud-filled region would also be set to 100%, typically only a small increase from the radiosonde-supplied value. For purposes of this study there are no actual clouds, but we will introduce a false cloud in some simulations to demonstrate how clear-sky errors influence liquid water retrievals. The relative humidity in the false cloud regions is not set to 100%. As with the vapor profile, this liquid water content profile is adjusted by a multiplicative value. If the input water profile is initially chosen as zero everywhere, than the iterative solution cannot find solutions with liquid water. The liquid multiplier when combined with the water content profile determines the cloud Liquid Water Path (LWP).

[23] The above approach reduces the problem of finding the PWV and LWP into a two-dimensional minimization problem. A number of different numerical schemes and associated cost (or minimization) functions can be used to solve this problem. We found that the traditional least absolute deviation was a satisfactory cost function, that is we seek the minimum of the function,

$$F(V,L) = \left|TB^{23}_{\text{calculated}}(V,L) - TB^{23}_{\text{measured}}\right| + \left|TB^{31}_{\text{calculated}}(V,L) - TB^{31}_{\text{measured}}\right|,$$

where, V and L are the vapor and liquid multiplicative factors and TB is either the measured or calculated brightness temperature at 23.8 or 31 GHz, as indicated by the associated subscripts. Choosing a minimization scheme was a little more difficult, because the function F does have a number of local minima. However, it turns out that if one fixes the value of L and then does a one-dimensional search in V, the minimum along this dimension is easy to find and is always in the trough where the global minimum can be found. We therefore choose to find the absolute minimum using nested one-dimensional searches. That is we find the minimum of the function $F(V_{\min}(L), L)$ where L is the only variable. $V_{\min}(L)$ is the value of V found at the minimum of $F(V, L)$

Table 1. Case Study Periods[a]

Date	Clear Periods, hours, UTC	Sonde Launches, hours and minutes, UTC	Notes and Instruments Used to Identify Clear Periods
		Tropical Western Pacific	
6/21/1999	10.2 to 12.35[b] 16.8 to 18.2[b]	5:38, 11:39, 17:34, 23:34	MPL, Radar, MWR
6/24/1999	8 to 10.2 10.6 to 11.8 16 to 20[c]	3:07, 5:26, 8:30, 11:30, 14:30, 17:29, 20:31, 23:20	MPL, VC, Radar, MWR, TSI & SW (after ~19.2)
7/03/1999	14.8 to 16.4 16.6 to 19.2 21.5 to 23.5[d]	5:30, 17:31, 23:42	MPL, Radar, MWR, TSI & SW (after ~19.2)
		Southern Great Plains	
3/04/2000	2 to 24	2:29, 5:32, 14:30, 17:30, 20:29, 23:32	MPL, Radar, MWR, TSI & SW (after ~13 UTC) near perfect skies!
3/08/2000	7.5 to 22	11:29, 14:34, 20:30, 23:29	MPL, Radar, MWR, TSI & SW (after ~13 UTC). Very thin and patchy cirrus move into area between 21 and 22 UTC
3/20/2000	13 to 23	2:32,14:30, 17:26, 20:28, 23:30	MPL, Radar, MWR, TSI & SW (after ~13 UTC). Some very light morning fog (or condensation on instruments) that cleared quickly after sunrise. Cirrus moves in late in the day.
		North Slope of Alaska	
5/13/2000	4 to 13	17:16 (5/12)	MPL, VC, Radar, MWR, SW (0 to 9 UTC). Radar shows some very weak detections at the surface between 6 & 10 UTC, but I believe this is just clutter which the automated clutter mask failed to remove. MPL shows weak but distinct aerosol layer from 1 to 1.2 km until 11 UTC when it ends abruptly.
8/15/2000	0 to 20	22:32 (8/14), 23:26 (8/15)	MPL, VC, Radar, MWR, SW (~0–7 & 14 to 20 UTC). Cirrus moves into area after 20 UTC becoming several km thick by end of day.
7/12/2001	2.5 to 24	23:01 (7/11), 22:59 (7/12)	MPL, VC, Radar, MWR, SW (~ 0 to 9.5 & 10.5 to 24) Near surface cloud clears after 2.5 UTC leaving clear sky for next 31+ hours
7/13/2001	0 to 10 15 to 19	22:59 (7/12), 22:58 (7/13)	MPL, VC, Radar, MWR, SW (~0 to 9.5 & 10.5 to 24) Cirrus observed by MPL and radar between 19–20 UTC. SW diffuse shows cloud effects between 10 & 15 UTC as well as after 19 UTC

[a]Definitions are as follows: VC, viasala ceilometer; MPL, micropulse lidar; Radar, 35 GHz cloud radar; MWR, microwave radiometer; SW, shortwave broadband direct & diffuse; TSI, total sky imager.
[b]VC shows some light activity, but the backscatter signal is too weak to be clouds.
[c]MPL shows thin (nearly subvisual) cirrus from ~16.5 UTC onward.
[d]TSI shows only a few cumulus (~5% coverage) with little impact on shortwave diffuse field.

with L fixed. No case was encountered where this approach failed.

4. Description of Cases

[24] A total of 10 days were selected for intensive study. Three of the days were selected from the ARM tropical western pacific (TWP) site at Nauru island, three are from the ARM southern great plains (SGP) site near Lamont Oklahoma, and four are from the ARM north slope of Alaska (NSA) site near Barrow. These 10 cases range in total precipitable water vapor from approximately 0.3 to 4.9 cm. In each case a variety of remote sensing instrumentation including a vaisala ceilometer, micropulse lidar, 35 GHz cloud radar, microwave radiometer, shortwave broadband radiometers (measuring both direct and diffuse flux) and at times a total sky imager (i.e., full-sky camera imagery) were examined to identify periods where the skies are clear of any clouds. Table 1 list the 10 days, the instruments used in determining that the sky were clear of clouds on each day, and the times when good quality radiosonde data was collected.

[25] For the SGP and TWP sites, the study periods were selected to occur during an ARM intensive operation period. During these periods, the ARM program launches 3 to 6 sondes a day and all the remote sensing instrumentation data is carefully evaluated. This was particularly valuable in regards to the TWP cases because other ship-based microwave radiometers were near the site at this time. All the ARM microwave radiometers use an automatic self-calibration algorithm [*Liljegren*, 2000]. Based in part on comparisons between radiometers and based in-part on a careful evaluation of the microwave radiometer tip-curve data, E. Westwater has concluded that the TWP radiometer calibration is good to 0.3 K or better at this time [*Westwater et al.*, 2003].

[26] The NSA cases were selected from a set of clear-sky days studied by *Barnard and Powell* [2002]. In their study of clear-sky surface shortwave fluxes, Barnard and Powell found that the NSA site did not appear to exhibit the so-called ''clear-sky diffuse field discrepancy,'' which had been reported at SGP and other midlatitude sites. The source of most of this discrepancy has subsequently been determined to be the result of an IR radiative effect within

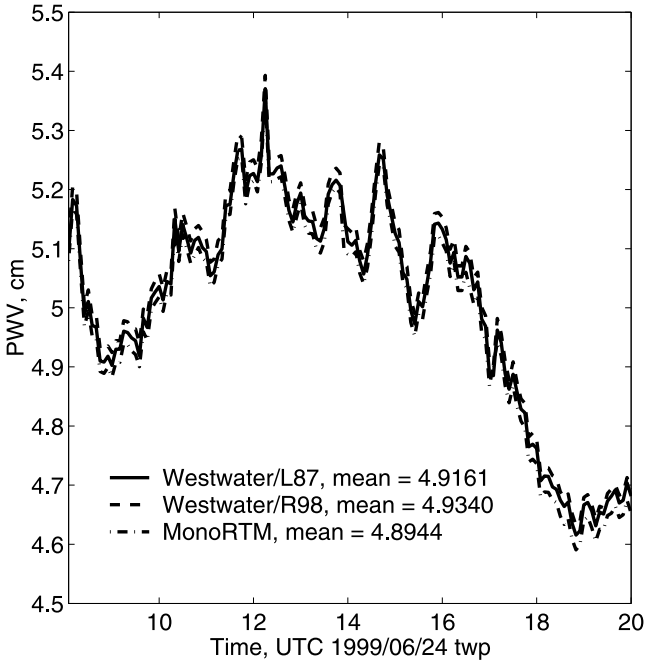

Figure 7. Precipitable water vapor obtained from clear-sky minimization.

the radiometers and has been corrected for in the SGP data sets. Barnard and Powell were able to calculate the downwelling direct and diffuse shortwave fluxes to better than 9 W/m^2 on average, lending additional credence to our claim that the cases examined here are clear of clouds.

5. Results

[27] In this section we examine in detail the results for one of the case study days. After this we present tables that summarizes the results for all 10 cases. As described in section 3, we use three different microwave absorption models: Liebe 1987, Rosenkranz 1998, and MonoRTM. We also examine two configurations, one in which the atmospheric column is not permitted to have any liquid water, we will refer to this as the clear-sky solution, and one in which it may have liquid water, but only in the region between 1 and 2 km above ground level.

[28] In the clear-sky or no-liquid-water solutions, the iterative solver is required to find the total column precipitable water vapor which minimizes the difference between the measured and a forward model calculation of the 23.8 GHz brightness temperature. In principle, the iterative solver can make this difference arbitrarily small. For purpose of this study difference was required not to exceed 0.05 K. Figure 7, shows the resulting precipitable water vapor required by each of the three models to match the measured 23.8 GHz brightness temperature. The difference in the results between the three models is less than 0.04 cm out of a total of approximately 4.9 cm. A residual difference of 0.03 to 0.04 was observed in all 10 cases.

[29] The purpose of the clear-sky solution is to evaluate the iterative solver's ability to calculate the brightness temperature at 31 GHz. Since there was no cloud and therefore no liquid water present during the measurement, if the microwave model and the atmospheric profile input are correct then the difference between the modeled and measured brightness temperature should be less than the accuracy of the 31 GHz measurement (about 0.3 K, in this case). Any disagreement between the modeled and measured values represent an error that would be introduced in determining the liquid water had a cloud been present.

[30] Figure 8 shows the difference between the model and measured microwave brightness temperature for one day at the ARM tropical western pacific site, Nauru. The downward spike just after 12 UTC is a cloud, and it is not included in the mean values shown in the legend. In this figure, as well as in all other figures and tables, the reported statistics are based only on the data in the clear-sky periods listed in Table 1. This figure shows that the all three solutions demonstrate a significant residual error. What is more disturbing is the approximately 1.3 K difference between the R98 and MonoRTM solutions. This is the largest differential between any of the solutions on any of the 10 cases examined in this study. The fact that this is the largest difference and that this is the case with the largest precipitable water vapor is not coincidental, as will be discussed later. In this case, the L87-based and MonoRTM-based solutions both appear to have underestimated the 31.4 GHz emissions, while the R98 model appears to have over-estimated the brightness temperature. The mean measured brightness temperature at 31 GHz during this time was 34.5 K (with a mean atmospheric radiating temperature of approximately 285.6 K and an

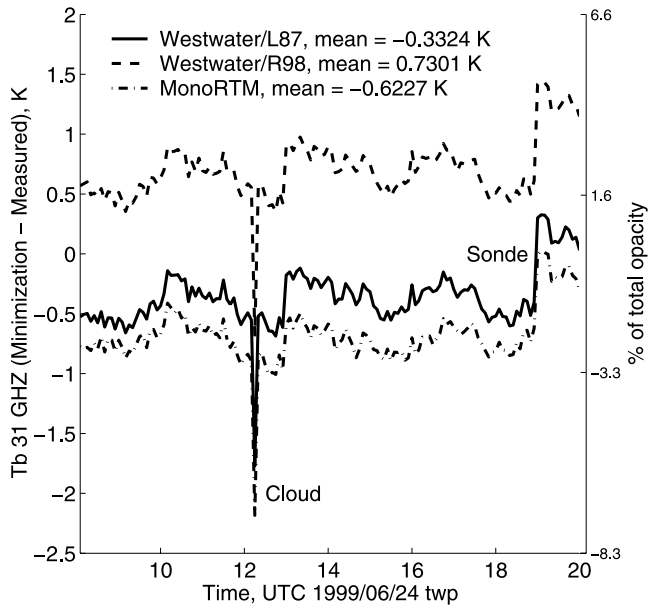

Figure 8. Difference between clear-sky calculated and measured 31.4 GHz brightness temperature. The downward spike just after 12 UTC is a cloud. The discontinuities near 13 and 19 UTC are due to choosing different radiosonde profiles. The mean values shown in the legend (as well as Tables 2 and 3) are based only on the known clear-sky periods listed in Table 1. To provide some measure of the relative size of these errors, consider the mean measured brightness temperature was 34.5 K and on the right axis the differences are given as the percentage of total opacity.

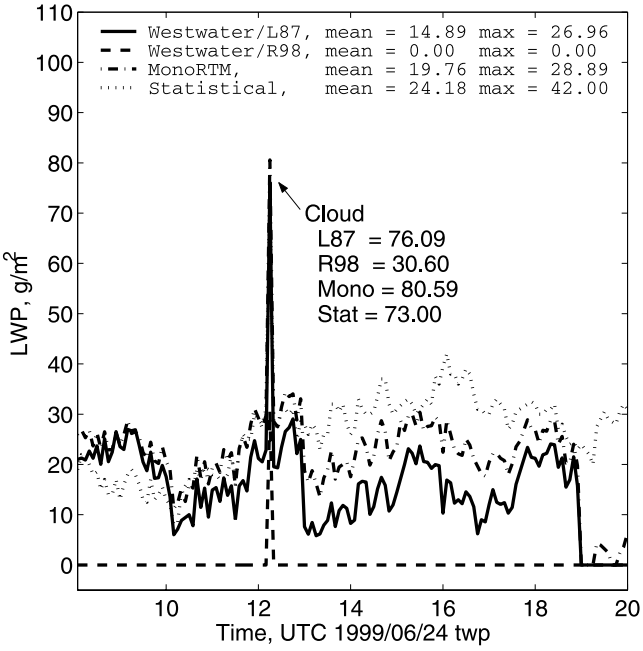

Figure 9. Retrieved column Liquid Water Path (LWP). Solutions based on the iterative solver require cloud to exists between 1 and 2 km above ground level. Also included is the ARM statistical retrieval for this same time period. The spike just after 12 UTC is caused by an isolated boundary layer cloud.

microwave opacity at 31 GHz of 0.12). Thus 1.3 K constitutes a relative difference of less than 5%, but as will be shown momentarily this is quite significant for the liquid water retrieval.

[31] A careful of examination of Figure 8, shows discontinuities in the residual error near 13 and 19 UTC. These jumps in the solution are due to switching between radiosonde profiles. As described in section 3, our iterative scheme uses the atmospheric profile from the nearest-in-time radiosonde. These jumps occur at the halfway points between sonde launches. It would have been simple to smooth over these jumps, for example, by linearly interpolating the atmospheric profiles in time. Rather, we have left this effect in the results to highlight the importance of the atmospheric profiles. Note that even at the times of the sonde launches (see Table 1 for launch times), all of the models show significant residual errors, often of more than 0.5 K. While Figure 8 shows that none of iterative solutions are in agreement with the measurements at 31.4 GHz, it is not clear whether the error is due to microwave absorption model or to the atmospheric profile inputs. What is clear is that all three microwave absorption models can not be correct.

[32] If we allow the iterative solver to seek solutions with liquid water, solutions with positive liquid water can be found when using the L87 or the MonoRTM models even when no clouds were present, as shown in Figure 9. In this case the solution using the L87 model yields an average liquid water path of about 15 g/m^2, while the MonoRTM model yields an average liquid water path of about 20 g/m^2. This is simply because the clear-sky solution based on these two models underestimated the total brightness temperature in the 31.4 GHz channel and so the calculations can be made to agree with the measurements (at both 23.8 and 31.4 GHz) by adding an additional source of microwave emissions, that is some liquid water. Since the R98 model has already overestimated the brightness temperature, adding more water doesn't help. However, this also means that the iterative scheme cannot make the measurements and calculation agree.

[33] The influence of these clear-sky errors in the 31.4 GHz calculations on an actual cloud water retrieval is demonstrated by the isolated boundary layer cloud which passed over the microwave radiometer just after 12 UTC. As the label in Figure 9 indicates, the R98 solution for the liquid water of this cloud is 30 g/m^2, whereas the L87 and MonoRTM solutions suggest the cloud has considerably more water. Because this particular cloud is so isolated, one can make a guess at its liquid water path from the L87 and MonoRTM solutions by subtracting the respective mean background in the "vicinity" of the cloud. Doing this suggests that this cloud had a LWP of roughly 50 to 55 g/m^2.

[34] Also included in Figure 9 are the results for the ARM statistical retrieval. As is apparent, the statistical retrieval is producing large and erroneous liquid water paths during the clear-sky periods on this day. This figure shows that the error in the statistical retrieval can be quite large, as much as 42 g/m^2 in this example, and we have observed what we believe to be errors as large as 60 g/m^2. This should not be taken to mean that the statistical retrieval usually produces such large errors (see Figure 6). We have also observed cases where the statistical retrieval produces extremely good agreement. It is largely a question of how close the actual atmospheric state is to effective-mean-state (in the set of data used to create the statistical retrieval coefficients) and whether or not the microwave absorption model used in the derivation of the statistical retrieval parameters is correct.

[35] The clear-sky error, such as that shown in Figure 8, can be further partitioned by examining the individual contributions of the water vapor continuum, water vapor line, and oxygen emission from the three models. Table 2 gives a breakdown of these components for a typical tropical atmosphere (4.2 cm of water vapor).

[36] Comparing L87 and MonoRTM models at 31.4 GHz (far right column, bottom half of the table) shows that the net difference between these two models is quite small

Table 2. Comparison of Brightness Temperature Components (Tropical Case)

	L87	R98	(L87-R98)	Mon	(L87-Mon)
			23.8 GHz		
No water (O2 & N2)	6.412264	6.83088	−0.41862	6.864768	−0.4525
Water line	56.89067	55.6661	1.224579	56.30751	0.583165
Water continuum	9.713808	10.62825	−0.91444	10.44495	−0.73114
Total water	62.54234	62.09543	0.446911	62.56958	−0.02724
All gases	65.43431	65.32559	0.108719	65.81454	−0.38023
			31 GHz		
No water (O2 & N2)	8.887909	9.447798	−0.55989	9.012545	−0.12464
Water line	14.75187	13.72796	1.023911	13.30171	1.450153
Water continuum	14.77109	16.33202	−1.56093	16.02435	−1.25326
Total water	26.2348	26.75505	−0.52025	26.05224	0.182554
All gases	31.83987	32.86258	−1.0227	31.77043	0.069447

Table 3. Difference Between Calculated and Measured Brightness Temperatures[a]

Date	Ave PWV, cm	(Calculated - Measured) L87	(Calculated - Measured) R98	31.4 GHz Temperature MonoRTM, K
		TWP		
1999 6 21	3.71	0.52(0.73)	0.43(0.63)	0.58(0.80)
1999 6 24	4.91	0.33(0.66)	0.73(1.45)	0.62(0.87)
1999 7 3	3.36	0.19(0.44)	0.79(1.17)	0.34(0.58)
		SGP		
2000 3 4	0.85	−0.02(−0.29)	0.42(0.66)	0.01(0.26)
2000 3 8	1.06	−0.14(−0.57)	0.32(0.57)	−0.03(−0.48)
2000 3 20	0.97	0.05(0.26)	0.51(0.70)	0.18(0.37)
		NSA		
2000 5 13	0.34	−0.73(−1.00)	−0.31(−0.58)	−0.92(−1.19)
2000 8 15	0.71	−1.06(−1.50)	−0.60(−1.03)	−1.07(−1.47)
2000 7 12	0.95	−0.61(−0.83)	−0.16(−0.38)	−0.62(−0.84)
2000 7 13	0.88	−0.74(−0.97)	−0.29(−0.52)	−0.73(−0.95)

[a]For each day and for each model the total atmospheric water vapor is determined by minimizing the 23 GHz measurements (as described in section 3). Ave PWV is the mean precipitable water vapor from the model solutions. Other columns show the mean difference (calculated - measured) in the 31 GHz channel were the mean is taken over the known clear-sky periods listed in Table 1. Values in parenthesis are the peak error (most negative or most positive, as appropriate) over this same period.

when all gasses are considered together (and hence the consistency between the results for these two models in Figures 8 and 9). Upon closer inspection, we can see that there are somewhat larger but offsetting differences in the oxygen and total water vapor components. Hidden within the total water vapor, the two models also have a notable difference in the division between the line and continuum contributions, which again largely offset each other.

[37] Comparing L87 and R98 models at 31.4 GHz (third column, bottom half of the table) shows the net difference between these two models is large. About half of the difference (0.5 K) is due to the background oxygen and half is due to water vapor (0.5 K). Recently, *Westwater et al.* [2001] independently identified this same background oxygen (or dry-atmosphere) offset in an analysis of data from the SHEBA experiment. As the column water vapor increases, the difference between the R98 and either the L87 or MonoRTM solution also increases.

[38] Table 3 provides a summary of the clear-sky 31 GHz residual errors for all 10 cases. The table shows that the L87 and MonoRTM models underestimated the clear-sky brightness temperature for both the tropical and artic cases, but did well for the midlatitude cases. The R98 model, on the other hand overestimated the tropical and midlatitude cases, but did well for the artic cases. Given the proceeding discussion on the contribution from the various gas components, it is not surprising that the largest inter-model difference occurs for the tropical cases, and that the midlatitude and arctic cases show much less inter-model differences with a typical offset of roughly 0.5 K (i.e., the background oxygen difference). While peak errors as large as ±1.5 K are observed, the error is usually less than 1 K.

[39] Table 4 gives a summary of the false-cloud retrieved liquid water path and mean total residual error. This table shows that underestimates in the 31 GHz brightness temperatures will yield erroneously large liquid water paths with a peak (worst) value over all 10 cases of 44 g/m^2, but with typical values ranging from 0 to 20 g/m^2. Combining the data from Tables 3 and 4 reveals that a 1 K error gives rise to a liquid water path error of approximately 30 g/m^2 (the full range is between 22 g/m^2 to 33 g/m^2 per degree Kelvin). Also shown in Table 4 are the results of the ARM programs statistical retrieval for these same cases. The ARM statistical retrieval is itself based on the L87 model, and a comparison of the statistical-approach results with the iterative solution based on the L87 model shows that the iterative solution did reduce the mean clear-sky errors for the tropical and midlatitude cases. For the artic cases, however, the iterative solution with the L87 model showed no improvement, although the R98 solution does.

6. Conclusions

[40] Retrievals of atmospheric liquid and water vapor based on passive microwave radiometers measurements

Table 4. Solution for Liquid Water Path (LWP)[a]

Date	L87 LWP, g/m^2	L87 R.E.	R98 LWP, g/m^2	R98 R.E.	MonoRTM LWP, g/m^2	MonoRTM R.E.	Statistical LWP
			TWP				
1999 6 21	21.72(30.16)	0.02	0.00(0.00)	0.44	19.47(26.87)	0.01	23.61(37.00)
1999 6 24	14.89(26.96)	0.05	0.00(0.00)	0.74	19.76(28.89)	0.03	24.18(42.00)
1999 7 3	8.21(17.13)	0.02	0.00(0.00)	0.80	10.09(20.00)	0.01	39.94(50.00)
			SGP				
2000 3 4	1.72(9.26)	0.04	0.00(0.00)	0.42	0.96(6.40)	0.04	4.96(13.00)
2000 3 8	4.51(18.13)	0.01	0.06(3.99)	0.32	1.79(14.38)	0.04	0.40(9.00)
2000 3 20	0.42(5.95)	0.07	0.00(0.00)	0.52	0.00(0.00)	0.20	−9.48(−4.00)
			NSA				
2000 5 13	16.16(22.28)	0.00	6.35(12.37)	0.00	19.28(24.95)	0.00	10.92(17.00)
2000 8 15	29.75(44.14)	0.00	16.78(30.33)	0.00	27.74(39.81)	0.00	14.56(25.00)
2001 7 12	17.64(24.23)	0.00	4.48(11.07)	0.01	16.23(22.46)	0.00	15.91(23.50)
2001 7 13	21.74(29.64)	0.00	8.43(15.64)	0.00	20.00(26.73)	0.00	16.10(21.00)

[a]Mean liquid water path retrieved when iterative code is permitted to find solutions with nonzero liquid water between 1 and 2 km above ground level. The mean is taken over the clear-sky periods listed in Table 1. Values in parenthesis are the maximum value of LWP over the same period. There is no cloud during these periods, such that the values shown indicated the level of overestimate in cloud LWP that would be expected had a cloud been present. R.E. is the residual or total brightness temperature error. A value of R.E. greater than 0.3 K indicates a significant error in model calculation, such that if a cloud had been present, its liquid water would be underestimated by more than 10 g/m^2.

are sensitive to variations in pressure and temperature of the liquid and water vapor in the atmospheric column. Retrieval of the column water vapor and the underlying microwave absorption models (near 23.8 GHz) appear quite good. This paper concentrates on problems associated with the retrieval of the column liquid water path as a result of uncertainties in the microwave emissions from oxygen and water vapor. We do not address here the uncertainty due to potential errors in the dielectric properties of water, which *Westwater et al.* [2001] have recently suggested may be a problem, especially for supercooled water. Nor has any consideration been given in this article to the uncertainties related to where one might choose to place the liquid water in the column (that is the liquid water temperature in the iterative solution), which is not necessarily obvious from radar or lidar data, especially for mixed phase clouds.

[41] An analysis of 10 clear-sky days showed differences between measured and modeled 31.4 GHz brightness temperatures typically agreed to better than ±1 K (equivalent to $\sim$30 g/m^2 in LWP), with the largest observed differences being near ±1.5 K. Errors were smaller near the time of sonde launches, but often remained more than 0.5 K. Changes from one sonde profile to the next generated occasional 0.5 to 1 K artifacts in the 31.4 GHz brightness temperature calculations, even when sonde launches were separated by only a few hours.

[42] This 10 case study is not sufficient to provide statistics on how well an iterative retrieval would do on the entire ARM data set. However, the above factors suggest that errors of 10 to 15 g/m^2 (0.5 K) will be common and occasional errors larger than 30 g/m^2 will occur. While the results in Table 4 suggest that the iterative solution will be an improvement over the traditional statistical retrieval, by more than a factor of 2 in some cases, the liquid water path error will remain significant for many clouds-as discussed in section 2.

[43] Particularly problematic is the 0.5 K to more than 1 K difference (depending on column water vapor) between the microwave absorption models at 31.4 GHz. The differences in the individual components (oxygen, water vapor line, self-broadened continuum, foreign-broadened continuum) are often larger than this but tend cancel out. Selecting one model over another represent not just an uncertainty, but a significant potential bias in the column liquid water retrieval. This bias is of the same magnitude as the uncertainty range suggested above. Indeed, the clear-sky results shown in Figure 6 indicate that such a bias does exist in clear-sky retrievals using the statistical method, although one cannot conclude from these data that the source of the bias is the microwave absorption model. In general we note that while the specific brightness temperature differences presented here were found using a physical-iterative, this uncertainly is fundamental to microwave radiative transfer.

[44] This is not the first study to point out disagreements between microwave absorption models and measurements [e.g., *Keihm et al.*, 2002; *Cruz-Pol et al.*, 1998; *Han et al.*, 1994]. It is our belief that the differences between the particular models shown here understate, rather than overstate, the true uncertainty in the microwave absorption model components at 31.4 GHz. It would be helpful to have an accurate assessment of the absorption model uncertainties starting from the laboratory data upon which these models were developed-not just best estimates of the absorption coefficients. Such uncertainty estimates could then in turn be used to determine the uncertainties in derived cloud liquid water due to the model.

[45] In any event, achieving an uncertainty of less than 10 g/m^2 will likely require both improvements in the atmospheric profile input (simple linear-interpolation of radiosonde data will not be sufficient) and significant reductions in the uncertainty of the microwave absorption model. Calibration of the MWR will also have to be maintained at a level of 0.3 K or better, even during cloud events that may occur many days from the nearest-in-time tip curve calibration.

[46] On the basis of analysis of an extensive ARM microwave radiometer data set, S. A. Clough et al. (manuscript in preparation) have implemented an empirical bias (zero water vapor, zero cloud) correction at each frequency. This effectively removes (1) modeling errors associated with dry air (oxygen/nitrogen) and (2) any offset brightness temperature error in the radiometer that is constant over time. Application of this offset bias provides significantly reduced cloud liquid water values under conditions of clear sky. It is also possible that improvements in the liquid water path retrieval cloud be made if measurements at additional microwave frequencies are included, but this remains a topic for further research.

[47] **Acknowledgments.** This research was supported by the Office of Biological and Environmental Research (OBER) of the U.S. Department of Energy as part of the Atmospheric Radiation Measurement (ARM) Program. The data presented here were collected by many people at different sites and distributed through the ARM archive. We are indebted to all the individuals involved in this process and offer our thanks.

References

Barnard, J. C., and D. M. Powell, A comparison between modeled and measured clear-sky radiative shortwave fluxes in Arctic environments, with special emphasis on diffuse radiation, *J. Geophys. Res.*, *107*(D19), 4383, doi:10.1029/2001JD001442, 2002.

Boukabara, S. A., S. A. Clough, and R. N. Hoffman, 2001 MonoRTM: A monochromatic radiative transfer model for microwave and laser calculation, paper presented at Specialist Meeting on Microwave Remote Sensing, Natl. Oceanic and Atmos. Admin., Boulder, Colo., 2001.

Clothiaux, E. E., T. P. Ackerman, G. G. Mace, K. P. Moran, R. T. Marchand, M. A. Miller, and B. E. Martner, Objective determination of cloud heights and radar reflectivities using a combination of active remote sensors at the ARM CART sites, *J. Appl. Meteorol.*, *39*(5), 645–665, 2000.

Clough, S. A., Y. Beers, J. Klein, and L. S. Rothman, Dipole moment of water from Stark measurements of H_2O, HDO, and D_2O, *J. Chem. Phys.*, *59*, 2254–2259, 1973.

Clough, S. A., F. X. Kneizys, and R. W. Davis, Line shape and the water vapor continuum, *Atmos. Res.*, *23*, 229–241, 1989.

Clough, S. A., M. J. Iacono, and J. L. Moncet, Line-by-line calculations of atmospheric fluxes and cooling rates: Applications to water vapor, *J. Geophys. Res.*, *97*, 15,761–15,785, 1992.

Cruz-Pol, S. L., C. S. Ruf, and S. J. Keihm, Improved 20- to 32-GHz atmospheric absorption model, *Radio Sci.*, *33*(5), 1319–1333, 1998.

Dong, X., T. Ackerman, and E. E. Clothiaux, Microphyscial and radiative properties of boundary later statiform clouds deduced from ground-based measurements, *J. Geophys. Res.*, *102*, 23,829–23,843, 1997.

Han, Y., and E. R. Westwater, Remote sensing of tropospheric water vapor and cloud liquid water by integrated ground-based sensors, *J. Atmos. Oceanic Technol.*, *12*(5), 1050–1059, 1995.

Han, Y., J. B. Snider, and E. R. Westwater, Observations of water vapor by ground-based microwave radiometers and Raman Lidar, *J. Geophys. Res.*, *99*, 18,695–18,702, 1994.

Hogg, D. C., F. O. Guiraud, J. B. Snider, M. T. Decker, and E. R. Westwater, A steerable dual-channel microwave radiometer for measurement of water vapor and liquid in the troposphere, *J. Appl. Meteorol.*, *22*(5), 789–806, 1983.

Keihm, S. J., Y. Bar-sever, and J. C. Liljegren, WVR-GPS comparison measurements and calibration of the 20–32 GHz tropospheric water vapor absorption model, *IEEE Trans. Geosci. Remote Sens.*, *40*(6), 1199–1210, 2002.

Liebe, H. J., An updated model for millimeter wave propagation in moist air, *Radio Sci.*, *20*(5), 1069–1089, 1985.

Liebe, H. J., and D. H. Layton, Millimeter wave properties of the atmosphere: Laboratory studies and propagation modeling, *Rep. 87-24*, Natl. Telecommun. and Inf. Admin (NTIA), Boulder, Colo., 1987.

Liebe, H. J., W. Rosenkranz, and G. A. Hufford, Atmospheric 60-GHz oxygen spectrum—New Laboratory Measurements and Line Parameters, *J. Quant. Spectrosc. Radiat. Transfer*, *48*(5–6), 629–643, 1992.

Liebe, H. J., G. A. Hofford, and M. G. Cotton, Propagation modeling of moist air and suspended water/ice particles and frequencies below 1000 GHz, *AGARD Conf. Proc.*, *542*(3), 1–3, 10, 1993.

Liljegren, J. C., Automatic self-calibration of ARM microwave radiometers, in *Microwave Radiometry and Remote Sensing of the Earth's Surface and Atmosphere*, edited by P. Pampaloni and S. Paloscia, pp. 433–443, VSP Press, 2000.

Liljegren, J. C., E. E. Clothiaux, G. G. Mace, S. Kato, and X. Q. Dong, A new retrieval for cloud liquid water path using a ground-based microwave radiometer and measurements of cloud temperature, *J. Geophys. Res.*, *106*, 14,485–14,500, 2001.

Min, Q., and L. C. Harrison, Cloud Properties derived from surface MFRSR measurements and comparison with GOES results at the ARM SGP site, *Geophys. Res. Lett.*, *23*(15), 1641–1644, 1996.

Rogers, R. R., and M. K. Yau, *A Short Course in Cloud Physics*, 3rd ed., Butterworth-Heinemann, Woburn, Mass., 1989.

Rosenkranz, W., Absorption of microwaves by atmospheric gases, in *Atmospheric Remotes Sensing by Microwaves*, edited by M. A. Janssen, pp. 37–90, John Wiley, Hoboken, N. J., 1993.

Rosenkranz, W., Water vapor microwave continuum absorption: A comparison of measurements and models, *Radio Sci.*, *33*(4), 919–928, 1998.

Rosenkranz, W., Correction to "Water vapor microwave continuum absorption: A comparison of measurements and models," *Radio Sci.*, *34*(4), 1025, 1999.

Schroeder, J. S., and E. R. Westwater, Users guide to WPL microwave radiative transfer software, *NOAA Tech. Mem. ERL WPL-213*, 1991.

Westwater, E. R., The Accuracy of water vapor and cloud liquid determinations by dual-frequency ground-based microwave radiometry, *Radio Sci.*, *13*(4), 677–685, 1978.

Westwater, E. R., Ground-based remote sensing of meteorological variables, in *Atmospheric Remotes Sensing by Microwaves*, edited by M. A. Janssen, pp. 145–213, John Wiley, Hoboken, N. J., 1993.

Westwater, E. R., Y. Han, M. D. Shupe, and S. Y. Matrosov, Analysis of integrated cloud liquid and precipitable water vapor retrievals from microwave radiometers during the Surface Heat Budget of the Arctic Ocean project, *J. Geophys. Res.*, *106*, 32,019–32,030, 2001.

Westwater, E. R., B. Boba Stankov, D. Cimini, Y. Han, J. A. Shaw, B. M. Lesht, and C. N. Long, Radiosonde humidity soundings and microwave radiometers during Nauru99, *J. Atmos. Oceanic Technol.*, *20*(7), 953–971, 2003.

T. Ackerman and R. Marchand, Pacific Northwest National Laboratory, P.O. Box 999, MSIN K9-38, Richland, WA 99352, USA. (roj@pnl.gov)

K. Cady-Pereira and S. A. Clough, Atmospheric and Environmental Research, 131 Hartwell Avenue, Lexington, MA 02421, USA.

J. C. Liljegren, Environmental Research Division, Argonne National Laboratory, 9700 South Cass Avenue, Building 203-CE111, Argonne, IL 60439, USA.

E. R. Westwater, Cooperative Institute for Research in Environmental Sciences, University of Colorado/NOAA Environmental Technology Laboratory, 325 Broadway MS R/E/ET1, Boulder, CO 80303, USA.